ACS APPLIED MATERIALS & INTERFACES

Research Article

www.acsami.org

Covalent Functionalization of Graphene Oxide with Biocompatible Poly(ethylene glycol) for Delivery of Paclitaxel

Zhiyuan Xu,[†,‡] Song Wang,[‡] Yongjun Li,*[,†] Mingwei Wang,[§] Ping Shi,*[,‡] and Xiaoyu Huang*[,†]

[†]Key Laboratory of Synthetic and Self-Assembly Chemistry for Organic Functional Molecules, Shanghai Institute of Organic Chemistry, Chinese Academy of Sciences, 345 Lingling Road, Shanghai 200032, People's Republic of China

[‡]State Key Laboratory of Bioreactor Engineering, East China University of Science and Technology, 130 Meilong Road, Shanghai 200237, People's Republic of China

[§]Department of Nuclear Medicine, Fudan University Shanghai Cancer Center, 270 Dongan Road, Shanghai 200032, People's Republic of China

ABSTRACT: Graphene oxide (GO), a novel 2D nanomaterial prepared by the oxidation of natural graphite, has been paid much attention in the area of drug delivery due to good biocompatibility and low toxicity. In the present work, 6-armed poly(ethylene glycol) was covalently introduced into the surface of GO sheets via a facile amidation process under mild conditions, making the modified GO, GO-PEG (PEG: 65 wt %, size: 50−200 nm), stable and biocompatible in physiological solution. This nanosized GO-PEG was found to be nontoxic to human lung cancer A549 and human breast cancer MCF-7 cells via cell viability assay. Furthermore, paclitaxel (PTX), a widely used cancer chemotherapy drug, was conjugated onto GO-PEG via $\pi-\pi$ stacking and hydrophobic interactions to afford a nanocomplex of GO-PEG/PTX with a relatively high loading capacity for PTX (11.2 wt %). This complex could quickly enter into A549 and MCF-7 cells evidenced by inverted fluorescence microscopy using Fluorescein isothiocyanate as a probe, and it also showed remarkably high cytotoxicity to A549 and MCF-7 cells in a broad range of concentration of PTX and time compared to free PTX. This kind of nanoscale drug delivery system on the basis of PEGylated GO may find potential application in biomedicine.

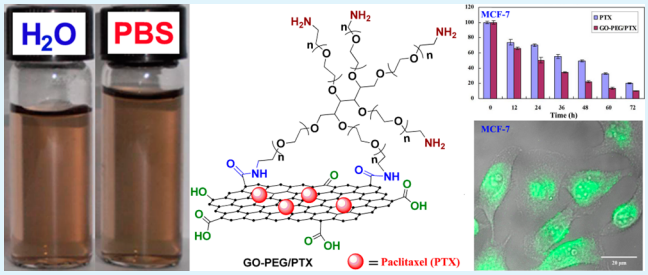

KEYWORDS: *graphene oxide, PEG, paclitaxel, A549, MCF-7*

INTRODUCTION

Graphene, a novel one-atom-thick two-dimensional graphitic carbon system, has opened up new opportunities in the field of nanotechnology and nanoscience since its first discovery in 2004.[1,2] As the basic building block of 0D fullerene, 1D carbon nanotubes, and 3D graphite,[3] its unique physical, chemical, and mechanical properties have attracted numerous investigations in recent years.[4−7] Potential applications of graphene in various fields, including nanoelectronic devices, sensors, solar cells, transparent conductors, and nanocomposite materials,[8−13] have been investigated extensively. Moreover, the applications of graphene and its oxidation derivative, graphene oxide (GO), in biological aspects such as drug loading and delivery, have also been intensively explored.[9,14,15] After oxidation, hydrophilic groups such as hydroxyl, carboxyl, and epoxy groups can be introduced onto the surface of GO sheets.[16,17] The existence of these oxygen-containing groups make GO stably suspend in pure water, yet GO will aggregate in solutions rich in salts or proteins such as cell medium and serum.[14] Furthermore, cytotoxicity tests have shown that graphene and GO exhibited a certain toxicity to cells and animals, while well-functionalized GO coated with biocompatible polymers was not obviously toxic in vitro and in vivo at the tested doses.[18−20] Therefore, the modification of GO through covalent or noncovalent functionalization, specifically, covalently grafting polymers onto GO sheets, is a significant step for biomedical applications.[21−24]

Poly(ethylene glycol) (PEG) is a very useful reagent in biology because of its minimal toxicity, biocompatibility, protein resistance, and good solubility in water or other common solvents.[25−29] The combination of PEG with other polymers or nanoparticles can effectively improve their biocompatibility.[30] The surface modification of nanoparticles with PEG has been widely employed in drug delivery systems.[31] The ultrahigh surface area of graphene is appropriate for loading of water-insoluble chemotherapy drugs.[14,32] Therefore, PEGylation of graphene would be a desired carrier for the delivery of hydrophobic anticancer drugs. Dai et al. initially developed PEG-functionalized nanoscale graphene oxide as a nanocarrier to load anticancer drugs via noncovalent physisorption and studied its cellular uptake.[9,14] They found that the modified nanosized graphene sheets were biocompatible without obvious toxicity and could load with aromatic anticancer drugs with high efficiency. Immediately after that, Chen et al. reported the in vitro binding and release of

Received: August 8, 2014
Accepted: September 12, 2014
Published: September 12, 2014

Scheme 1. Preparation of GO-PEG/PTX Nanoscale Drug Delivery System

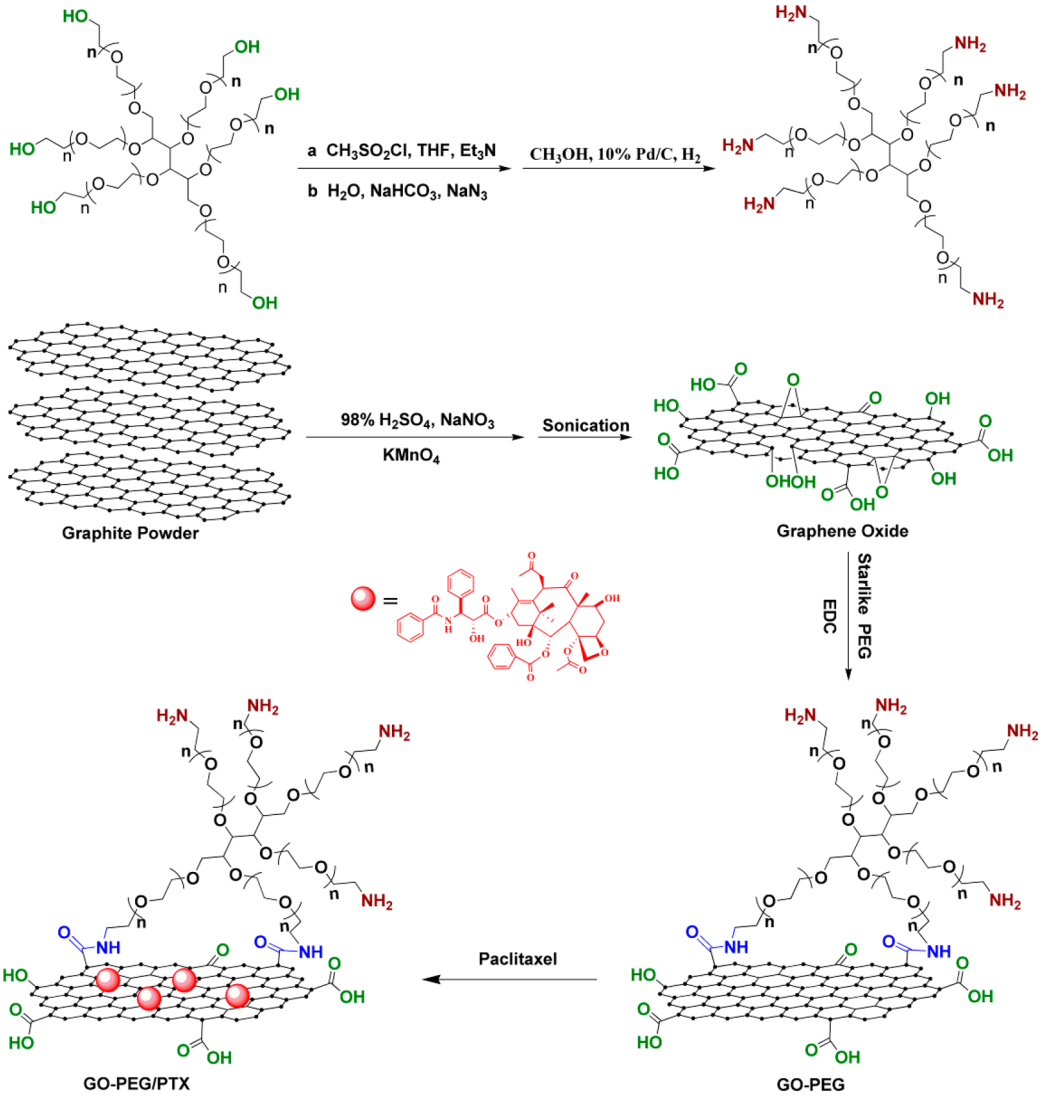

doxorubicin hydrochloride (DOX) on GO sheets, and found that the loading ratio of DOX was significantly high and dependent on pH value.[32]

Paclitaxel (PTX) is a commonly used potent chemotherapy drug which shows high cytotoxicity to cancer cells.[33] PTX was considered as the most significant progress in tumor chemotherapy in recent decades by National Cancer Institute (NCI), since it was extracted from taxus drevifolia.[34] However, the low water solubility, poor bioavailability, and emergence of drug resistance in patients limited the biological application of PTX.[35,36] In this paper, we proposed a new GO-based drug delivery system as shown in Scheme 1 for cancer therapy to improve the utilization rate of PTX. We first prepared GO by a modified Hummer's method, and then modified GO through grafting biocompatible 6-armed starlike PEG and linear PEG to render the aqueous stability and biocompatibility. The starlike PEG modified GO, GO-PEG, showed good stability both in water and PBS buffer after one month. The successful functionalization of GO was verified by FT-IR, atomic force microscopy (AFM), thermogravimetry analysis (TGA), and elemental analysis. Next, PTX was physically loaded onto GO-PEG nanocarrier via $\pi-\pi$ stacking and hydrophobic interactions to afford a nanosized complex, GO-PEG/PTX. This nanocomplex could be efficiently taken up by A549 lung cancer cells and MCF-7 breast cancer cells from the intracellular imaging. It was found from cell viability assay that GO-PEG/PTX could be a highly potent killer of cancer cells in vitro with a higher cytotoxicity to A549 and MCF-7 cells compared to free PTX. This way could significantly improve the bioavailability of PTX as well as other hydrophobic drugs.

EXPERIMENTAL SECTION

Materials. Six-armed PEG with six hydroxyl end groups (6-armed PEG−OH, M_n = 5300 g/mol determined by MALDI-TOF-MS, M_w/M_n = 1.04 determined by GPC) was synthesized by anionic polymerization of ethylene oxide using D-mannitol as initiator.[37] Graphite powder (Aldrich, 99.99+%), HO-PEG−OH (Aldrich, average M_w = 1500 g/mol), fluorescein isothiocyanate (FITC, Aldrich, 90%), paclitaxel (PTX, Aldrich, 99%), sulfuric acid (H_2SO_4, Aldrich, 95−98%), sodium nitrate ($NaNO_3$, Aldrich, 99%), *N*-(3-(dimethylamino)propyl)-*N*′-ethylcarbodiimide hydrochloride (EDC·HCl, Aldrich, 99%), potassium permanganate ($KMnO_4$, Aldrich, 99%), and cell counting kit-8 (CCK-8, Dojindo, Japan) were used as received. RPMI 1640 and DMEM medium were purchased from GIBCO/Invitrogen, U.S.A., and supplemented with 10% fetal bovine serum (FBS, BI Biological Industries Ltd., Israel) and 1% penicillin-streptomycin (10 000 U/mL penicillin and 10 mg/mL streptomycin,

dx.doi.org/10.1021/am505308f | ACS Appl. Mater. Interfaces 2014, 6, 17268−17276

Solarbio Life Science, China). Six-armed PEG−OH and HO-PEG−OH were converted to 6-armed PEG with six amino end groups (6-armed PEG-NH_2) and H_2N-PEG-NH_2 according to previous literature[38] as shown in Scheme 1.

Measurements. FT-IR spectra were recorded on a Nicolet AVATAR-360 FT-IR spectrophotometer with a resolution of 4 cm^{-1}. UV−vis spectra were measured by a Hitachi U-2910 spectrophotometer. Absolute number-average molecular weight was determined by MALDI-TOF-MS using an Applied Biosystems Voyager DE-STR spectrometer. Molecular weight distribution was measured by conventional GPC system equipped with a Waters 1515 Isocratic HPLC pump, a Waters 2414 refractive index detector, and a set of Waters Styragel columns (HR3 (500−30 000), HR4 (5000−600 000), and HR5 (50 000−4 000 000), 7.8 × 300 mm^2, particle size: 5 μm). GPC measurement was carried out at 35 °C using THF as eluent (flow rate: 1.0 mL/min). Atomic force microscopy (AFM) images were taken by a Veeco DI MultiMode SPM in the tapping mode of dropping the sample solution onto the freshly exfoliated mica substrate. Thermogravimetry analysis (TGA) measurements were run on a TA Q500 system under N_2 purge with a heating rate of 10 °C/min. Elemental analysis was carried out on an Elementar Vario EL III system. The relative cell viability was measured at the absorbance of 450 nm using a Tecan GENios Pro microplate reader. Cellular uptake images were taken by an Olympus BX51 fluorescence microscope.

PREPARATION OF GRAPHENE OXIDE

GO was prepared from graphite powder through a modified Hummer's method.[4] Graphite powder was oxidized by neat H_2SO_4 and $KMnO_4$ with three different stages and followed by filtration and subsequently dialysis against deionized water for several days to remove residual salts and acids. Finally, the obtained GO aqueous dispersion (0.1 mg/mL) was exfoliated by water-bath ultrasonication for 3 h, and the supernatant was obtained, which would not precipitate for several months.

PREPARATION OF GO-PEG AND GO-PEG1500

GO was first dispersed in double-distilled water followed by adding 6-armed PEG-NH_2 and EDC·HCl for sonication at room temperature for 1 h. The solution was kept stirring vigorously at room temperature overnight. The final product, GO-PEG, was obtained by purifying the crude product by dialysis (MW cutoff = 14 kDa) against double-distilled water for 1 week to remove unbound 6-armed PEG-NH_2. H_2N-PEG-NH_2 was also covalently linked to GO using the similar method (dialysis: MW cutoff = 3.5 kDa) to afford the corresponding product, GO-PEG1500.

Cell Culture. Human lung cancer A549 and human breast cancer MCF-7 cells were supplied by Shanghai Institute of Cell Biology, Chinese Academy of Sciences. They were cultured at 37 °C under a humid 5% CO_2 atmosphere in RPMI 1640 and DMEM medium, respectively, supplemented with 10% FBS and 1% penicillin-streptomycin.

Cellular Uptake of GO-PEG. GO-PEG was labeled by FITC by mixing 1 mL of FITC aqueous solution (0.5 mg/mL) with 8 mL of GO-PEG aqueous suspension (3.5 mg/mL). Free FITC was removed by dialysis against double-distilled water for 48 h. The resulting fluorescein labeled GO-PEG, GO-PEG/FITC nanocomplex was stored at 4 °C. A-549 and MCF-7 cells were plated on a 20 mm glass round coverslip in 6-well plates, and allowed to adhere overnight. A549 and MCF-7 cells were incubated with GO-PEG/FITC nanocomplex for 1, 3, and 6 h and washed with PBS three times. The cells were then imaged under an inverted Olympus BX51 fluorescence microscope.

LOADING OF PTX ON GO-PEG

PTX solution (0.5 mg/mL, solvent: DMSO, 10 mL) was added to 10 mL of GO-PEG aqueous dispersion (0.5 mg/mL), and the mixture was stirred at room temperature for 24 h. Excess precipitated PTX was removed by repeated centrifugation at 4000 rpm. The solution was then filtered through a filter (MW cutoff = 10 kDa) and repeatedly washed with double-distilled water to remove DMSO and small amount of solubilized free PTX. The formed GO-PEG/PTX nanocomplex was stored at 4 °C. The loading ratio of PTX (wt %) was determined from UV absorbance at 229 nm after deducting the absorbance of GO-PEG at 229 nm.

In Vitro Cell Viability Assay. A549 and MCF-7 cells were plated in 96 well plates at a density of 5 × 10^3 cells per well in 100 μL culture medium (RPMI 1640 for A549 and DMEM for MCF-7) and added with desired concentrations of GO, GO-PEG, GO-PEG/PTX, and free PTX (dissolved in DMSO and diluted in PBS). The relative cell viability was measured by WST assay using CCK-8. After continuous incubation for 12, 24, 36, 48, 60, and 72 h, absorbance was measured at 450 nm using a Tecan GENios Pro microplate reader.

Statistical Analysis. Values were expressed as means ± standard deviations. Statistical analysis was performed using the Student's t test. Values of $p < 0.05$ were considered to be statistically significant.

RESULTS AND DISCUSSION

Preparation and Characterization of GO-PEG. The modified Hummer's method was first employed to prepared graphite oxide using natural graphite powder as starting material.[4] Graphite oxide certainly bears many oxygen-containing groups including carboxyls at the edge, hydroxyls, and epoxy groups on the basal plane[32] produced by oxidation process. Graphite oxide is usually employed as the starting functional precursor because oxygen-containing groups on its surface provide reactive sites for the succedent covalent modification such as the esterification of carboxyls or ring-opening reaction of epoxy groups.[17,39] The aqueous dispersion of graphite oxide was then exfoliated by water bath ultrasonication to afford GO. The existence of oxygen-containing groups on the surface of GO was examined by FT-IR (Figure 1) and element analysis (Table 1). The strong and broad peak

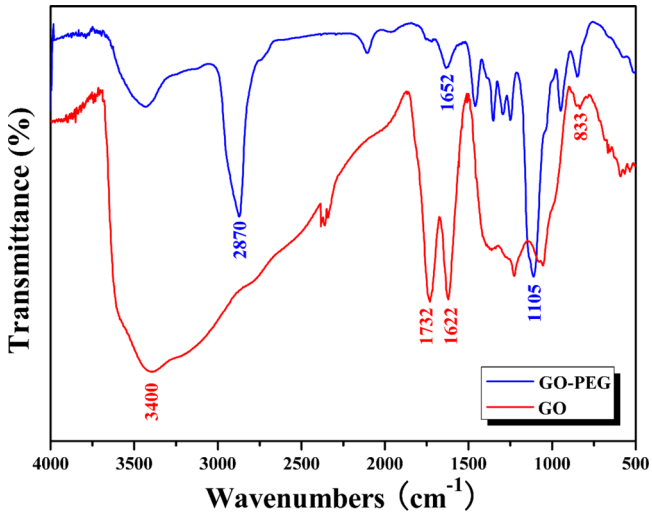

Figure 1. FT-IR spectra of GO and GO-PEG.

Table 1. Element Analysis of Graphite Powder, GO, and GO-PEG

sample	C (wt %)	H (wt %)	O (wt %)	N (wt %)
graphite powder	97.8	0.6	1.6	0
GO	47.4	3.4	49.2	0
GO-PEG	53.9	7.7	36.5	1.9

around 3400 cm^{-1} in FT-IR spectrum (Figure 1) was attributed to hydroxyls and carboxyls while the sharp peak at 1732 cm^{-1} was originated from the carbonyls in carboxyls. The characteristic signal at 833 cm^{-1} verified the presence of epoxy groups. The peak at 1622 cm^{-1} corresponded to the vibration of undried water molecules, and these undried water molecules also contributed to the strong and broad peak at 3400 cm^{-1}. Table 1 shows the results of element analysis before and after the oxidation process. It can be found from the table that the oxygen content was found to be greatly increased to 49.2 wt % after the oxidation, compared to the value of 1.6 wt % before oxidation, which clearly evidenced a high degree of oxidation with the existence of many oxygen-containing groups on the surface of GO sheets. In particular, it should be noted that the content of nitrogen was still 0% after the oxidation.

The stability of GO was tested in aqueous media and PBS solution. GO was found to be stable in water for 30 days without precipitation (Figure 2A). However, it aggregated and

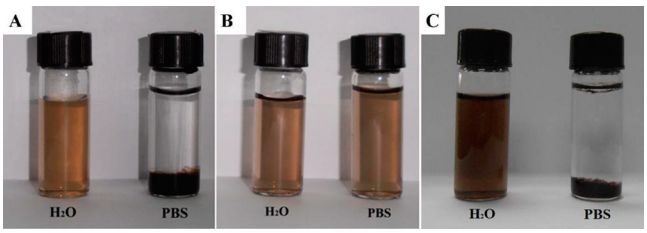

Figure 2. Colloidal stability of GO (A), GO-PEG (B), and GO-PEG1500 (C) in water and PBS solution after placing 30 days.

precipitated in PBS solution (Figure 2A), clearly implying the necessity for improving the stability of GO under physiological conditions for further application in biomedicine.

Therefore, we utilized anionic polymerization technique to synthesize a well-defined 6-armed PEG−OH with an absolute number-average molecular weight of 5300 g/mol and a narrow molecular weight distribution of 1.04, since PEG is well known to be biocompatible. The six terminal hydroxyls could certainly react with carboxyls in the surface of GO sheets via esterification so that biocompatible PEG chains could be linked onto the surface of GO sheets via stable covalent bonds. However, the reaction conditions of esterification were relatively violent, including strong acid (H_2SO_4) and high temperature. Thus, in order to facilitate the covalent grafting of PEG chains onto GO surface, 6-armed PEG−OH was transformed into 6-armed PEG-NH_2 so that six terminal amino groups with higher reactivity could readily react with carboxyls in the surface of GO sheets via amidation. Indeed, the amidation process was performed smoothly at ambient temperature in aqueous media.

After the amidation reaction, the sharp peak at 1732 cm^{-1} in FT-IR spectrum before the amidation completely disappeared and a new signal originating from amide group (—NH—CO) appeared at 1652 cm^{-1} in FT-IR spectrum after the amidation (Figure 1) instead. This evidence distinctly demonstrated that the initial carboxyls on the surface of GO sheets were entirely converted to amide groups. The presence of amide groups was also verified by element analysis since that the content of nitrogen (0% before the amidation) was increased to 1.9 wt % (Table 1) after the amidation. Both points sufficiently showed the covalent grafting of PEG chains onto the surface of GO sheets. Meanwhile, another two strong peaks at 2870 cm^{-1} (—CH_2—) and 1105 cm^{-1} (—C—O—) also definitely illustrated the existence of PEG chains on the surface of GO sheets. For comparison, linear H_2N−PEG−NH_2 with a weight-average molecular weight of 1500 g/mol was also covalently functionalized onto the surface of GO sheets using the same approach to afford the product of GO-PEG1500.

The ratio of grafted PEG was determined by TGA. As a complementary technique, TGA could reveal the composition and thermal stability of GO-PEG and GO-PEG1500. Figure 3

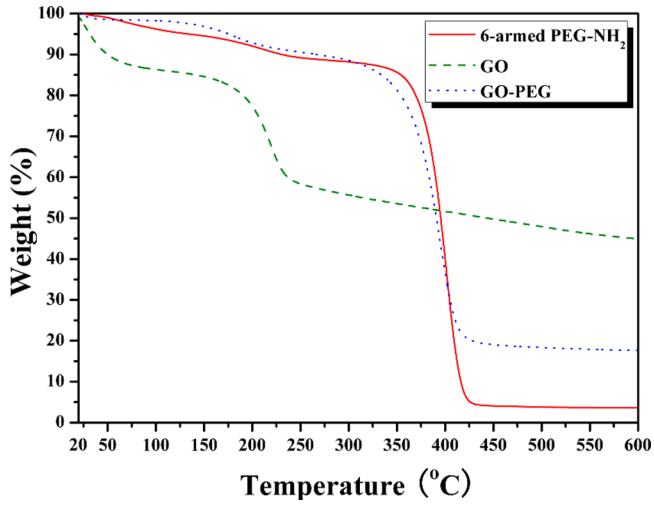

Figure 3. TGA (in N_2) curves of GO, 6-armed PEG-NH_2, and GO-PEG with a heating rate of 10 °C/min.

shows TGA curves of raw materials for amidation, GO, and 6-armed PEG-NH_2, and the resulting product of amidation, GO-PEG. It can be seen from the figure that GO was thermally unstable, and it began to lose mass below 100 °C due to the volatilization of stored water in the π-stacked structure.[4,39] The mass loss was remarkably accelerated in the range of 170 to 230 °C because of the pyrolysis of labile oxygen-containing groups.[4,39] PEG polymeric coatings seemed to be effective for enhancing the thermal stability of GO sheets. The mass loss of GO-PEG was obviously accelerated from 350 °C, which was nearly 180 °C higher than that of GO. TGA data indicated that GO-PEG had a 82.4% weight loss at 600 °C in N_2, while the values for GO and 6-armed PEG-NH_2 were 55.0% and 96.4%, respectively. So, it was estimated according to the following equation set (x and y are weight percentage of GO and PEG, respectively.) that GO-PEG contained about 33.8 wt % of GO and 66.2 wt % of PEG. Furthermore, the weight loss at 600 °C in N_2 for GO-PEG1500 and H_2N-PEG-NH_2 were 67.6% and 98.2%, respectively. Then, GO-PEG1500 was evaluated to bear about 70.8 wt % of GO and 29.2 wt % of PEG.

$$0.55x + 0.964y = 0.824 \quad (1)$$

$$x + y = 1 \quad (2)$$

Both PEG-functionalized GO could well disperse in water even after 30 days as shown in Figure 2B,C. The stability of

GO-PEG in PBS solution was much superior to GO and GO-PEG with a higher weight ratio of PEG (66.2 wt %) could well disperse in PBS solution even after 30 days without precipitation (Figure 2B). However, GO-PEG1500 with a lower weight ratio of PEG (29.2 wt %) was found to aggregate and precipitate in PBS solution after 30 days (Figure 2C). This phenomenon clearly indicated that the stability of GO under physiological conditions definitely depended on the content of grafted PEG, more grafted hydrophilic and biocompatible PEG would result in better stability in PBS solution.

The morphology of GO before and after bonding with PEG was visualized by AFM, as shown in Figure 4. The measured thickness of GO sheets remained at 0.8−1.4 nm with a smooth surface (Figure 4A), which was consistent with previous reports;[9,14] yet it acutely increased to 1.6−3.5 nm (Figure 4B) after the amidation with 6-armed PEG-NH_2. The surface of GO-PEG was relatively rough with some protuberances (Figure 4B), mainly due to the attachment of PEG onto both planes of GO sheets.

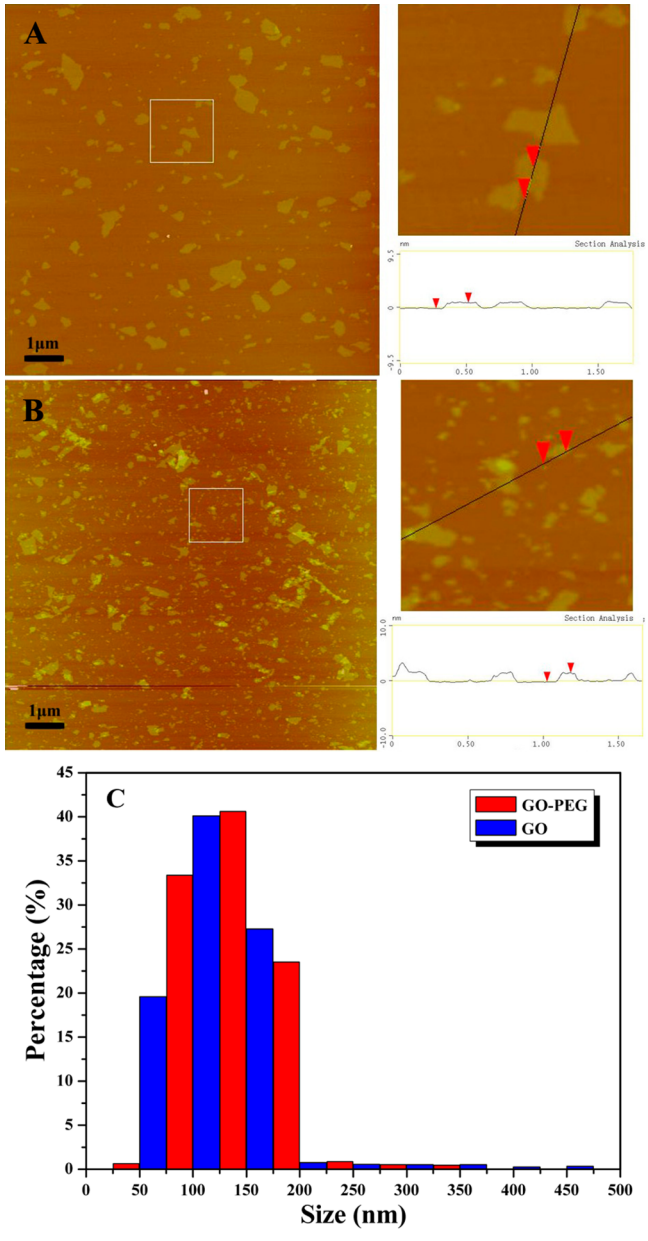

Figure 4. AFM images of GO (A), GO-PEG (B), and size statistical graph (C).

Both GO and GO-PEG sheets had a lateral size ranging from 50 to 200 nm (Figure 4C), and this size surely could benefit the application of GO-PEG for drug delivery due to the well-known enhanced permeability and retention (EPR) effect.[40] Thus, as a potential nanocarrier, GO-PEG with a reasonable dimension was very suitable for drug delivery.

Cellular Uptake of GO-PEG. In order to affirm whether GO-PEG carrier could readily enter cells, we used FITC as a fluorescent probe for intracellular imaging.[41] FITC was mixed with GO-PEG in aqueous media to form covalently bonded complex, GO-PEG/FITC.[42] Figure 5 shows UV−vis absorbance spectra of GO-PEG before and after mixing with FITC. UV−vis absorbance spectrum of GO-PEG was almost a smooth curve in the range of 200 to 700 nm without any distinct absorption peak. However, after mixing with FITC, the spectrum showed a sharp absorption peak at 488 nm originated from FITC, indicating the successful binding of FITC to GO-PEG for affording the resulting FITC-labeled GO-PEG nanocomplex, GO-PEG/FITC.

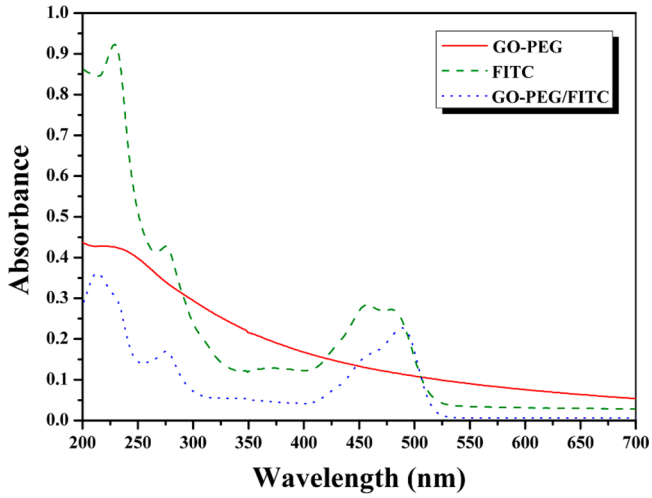

Figure 5. UV−vis absorbance spectra of FITC before and after mixing with GO-PEG.

We then investigated the cellular uptake of GO-PEG/FITC by incubating A549 and MCF-7 cells with GO-PEG/FITC for fluorescence imaging. As shown in Figure 6, fluorescence were observed in both A549 and MCF-7 cells, which clearly demonstrated that GO-PEG penetrated cell membranes and entered cells. Thus, we can confirm the cellular uptake of GO-PEG by A549 and MCF-7 cells.

Cytotoxicity of GO-PEG and PTX Loading on GO-PEG. To make sure whether GO-PEG nanocarrier is nontoxic to A549 and MCF-7 cells, WST-8 based colorimetric assay was employed to detect the cytotoxicity effect of GO-PEG on A549 and MCF-7 cells. A549 and MCF-7 cells were first incubated in a suitable medium (RPMI 1640 for A549 and DMEM for MCF-7) containing various concentrations of GO-PEG. As shown in Figure 7, high cell viability (>85%) for both A549 and MCF-7 cells were found for various concentrations of GO-PEG after incubating 72 h, even at a high concentration of 100 mg/L, which illustrated that GO-PEG nanocarrier was not cytotoxic by itself.

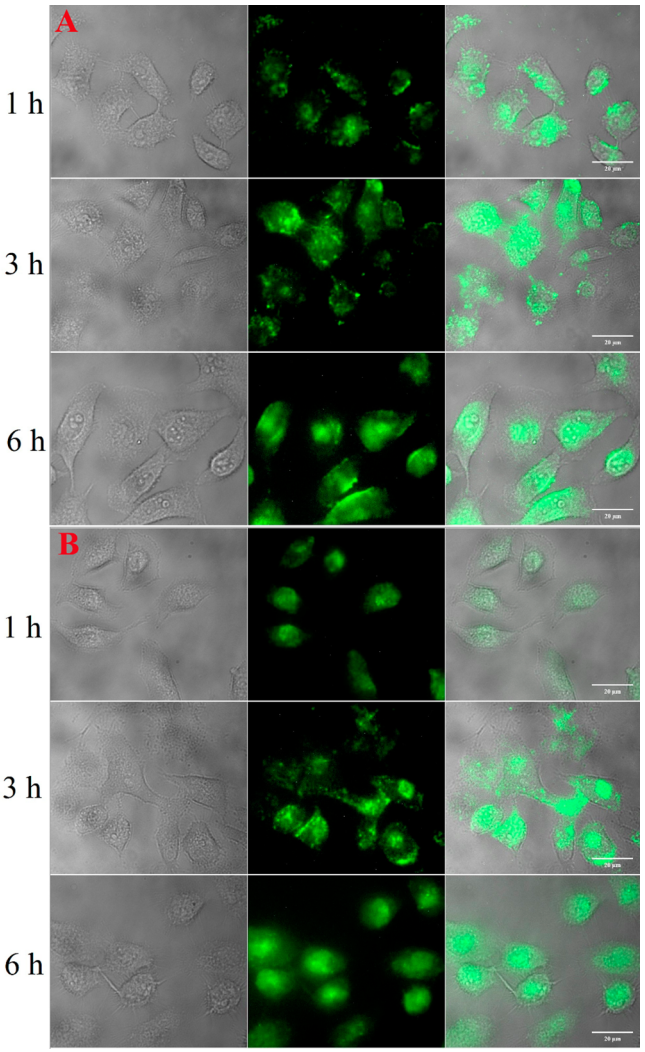

Figure 6. Differential interference contrast (left), fluorescence (center), and merge (right) images of A547 (A) and MCF-7 (B) cells incubated with GO-PEG/FITC for 1, 3, and 6 h, respectively. Scale bar: 20 μm.

As we know, many anticancer drugs such as PTX and CPT are aromatic and hydrophobic. Owing to the poor water solubility, their clinical applications are obviously limited. The large π-conjugated structure of GO can form $\pi-\pi$ stacking interaction with these aromatic drugs and two planes of GO can both adsorb aromatic compounds, which suggests potential application as a drug carrier. Moreover, recent reports declared that 2D shape and ultrasmall size of PEGylated graphene sheets showed interesting in vivo properties, including highly efficient passive tumor targeting and relatively low retention in reticuloendothelial systems.[33,43] Herein, we chose PTX as a model drug to form GO-PEG/PTX nanocomplex for increasing the utilization rate of PTX.

The loading of PTX on GO-PEG was achieved by mixing PTX (dissolved in DMSO) with GO-PEG aqueous suspension directly. The unbound or undissolved PTX was removed by centrifugation and filtration. The successful loading of PTX on GO-PEG was evidenced by the characteristic absorption peak at 229 nm (originating from PTX) in UV–vis absorbance spectrum of GO-PEG after mixing with PTX (Figure 8B), which was absent in that before mixing with PTX (Figure 8B). To determine the loading ratio of PTX on GO-PEG, the standard absorption of PTX at 229 nm was plotted in the inset of Figure 8A according to UV–vis absorbance spectra of PTX with various concentrations in Figure 8A. So, the absorbance of loaded PTX at 229 nm could be obtained by subtracting the absorbance of GO-PEG at 229 nm from that of nanocomplex, GO-PEG/PTX, at 229 nm. The load capacity (weight ratio of loaded PTX to GO-PEG nanocarrier) was estimated to be 11.2 wt % via the standard absorption of PTX at 229 nm. As previously stated, no drug was loaded on PEG in a solution free of GO in a control experiment,[14] therefore, PTX loading was all owed to GO. Due to the lack of chemical reaction between PTX and GO-PEG, physical adsorption of PTX could preserve its biological activity in comparison with the drug loading on carrier via covalent bond.

The cytotoxicity effect of GO-PEG/PTX nanocomplex on A549 and MCF-7 cells was also detected using WST-8 based colorimetric assay as shown in Figure 7. It was found that the cell viability of A549 and MCF-7 cell after incubating with GO-PEG/PTX for 72 h were as low as 32.1% and 9.7%, respectively, even with a low concentration of 1.29 mg/L for

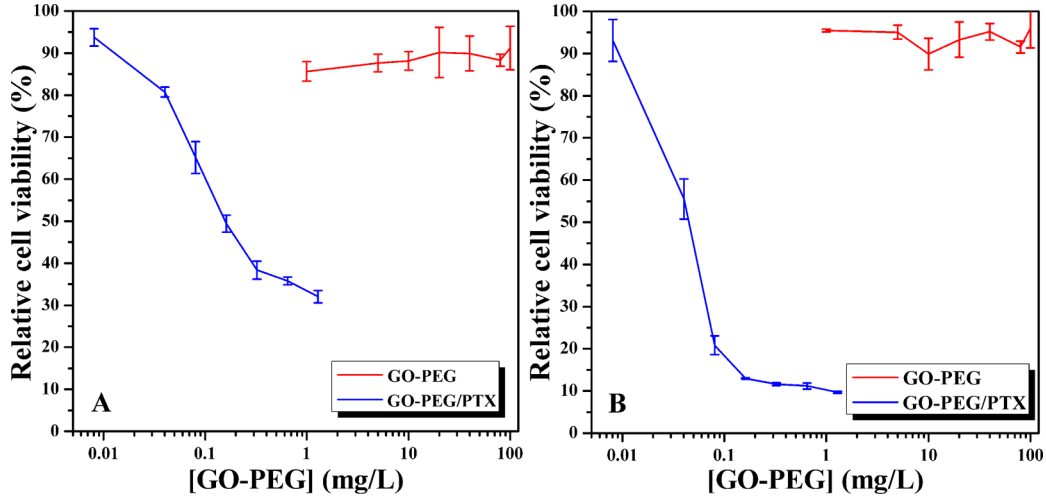

Figure 7. Relative cell viability of A549 (A) and MCF-7 (B) cells after incubating with GO-PEG and GO-PEG/PTX for 72 h. Error bars were based on triplet samples.

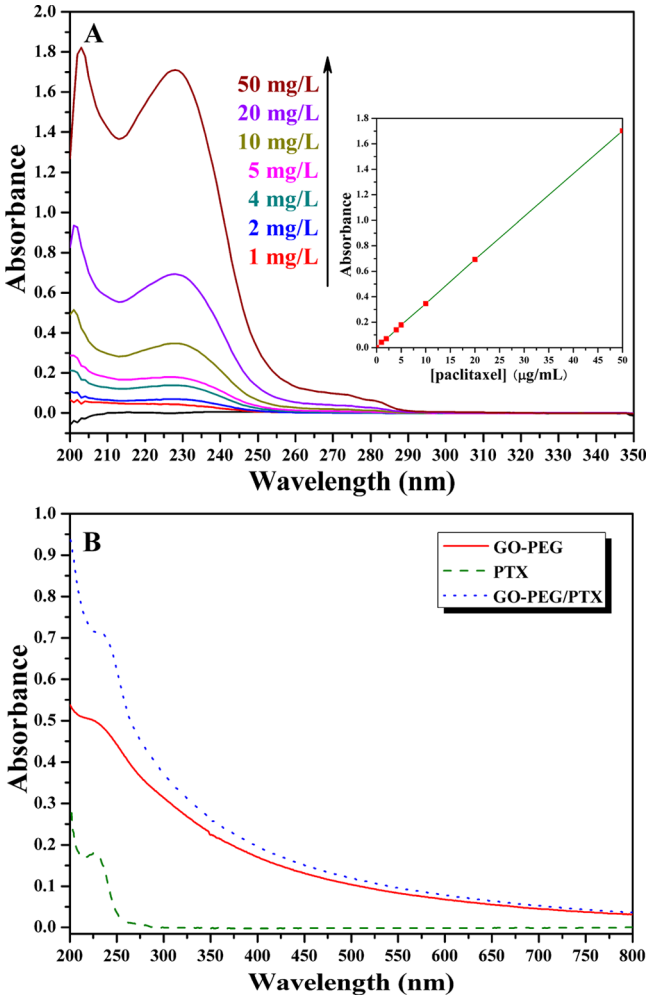

Figure 8. (A) UV−vis absorbance spectra of PTX with different concentrations and UV−vis absorbance standard curve of PTX at 229 nm (inset). (B) UV−vis absorbance spectra of GO-PEG before and after loading PTX.

GO-PEG, compared to the much higher cell viability for both A549 (91.2%) and MCF-7 (95.9%) cells even with a high concentration of 100 mg/L for GO-PEG. Thus, it can be concluded that the cytotoxicity of GO-PEG/PTX nanocomplex was caused by the carried PTX only.

In Vitro Cell Toxicity of GO-PEG/PTX. In the current case, cytotoxicity effects of GO-PEG/PTX nanocomplex and free PTX on A549 and MCF-7 cells were examined by WST-8 based colorimetric assay. Figure 9A,B shows the relative cell viability of A549 and MCF-7 cells after incubating with PTX and GO-PEG/PTX for 72 h while varying the concentration of PTX. Both free PTX and GO-PEG/PTX inhibited A549 and MCF-7 cells in a time-dependent manner and the relative cell viability obviously declined with the rising of PTX concentration. When the PTX concentration was very low (≤1 nM), cytotoxicity effects of GO-PEG/PTX and free PTX on both A549 and MCF-7 cells were similar, the cell viabilities were all higher than 93% and the margins were very small (<5%). However, GO-PEG/PTX clearly exhibited a higher cytotoxic effect on tumor cells compared to free PTX with increasing PTX concentration. For instance, A549 cell viabilities were 82.5% for free PTX and 49.4% for GO-PEG/PTX with a PTX concentration of 20 nM; MCF-7 cell viabilities were 47.7% for free PTX and 12.9% for GO-PEG/PTX with a PTX concentration of 20 nM. Because MCF-7 cell was much sensitive to PTX than A549 cell, it showed a higher cytotoxicity effect than A549 cell with the same drug concentration at a comparable incubation time. The disparity of relative cell viability after incubating with free PTX and GO-PEG/PTX decreased at high PTX concentrations (>80 nM) owing to the drastic toxicity of drug to cells at high concentrations. Moreover, it was worth pointing out that GO-PEG/PTX with a low concentration of PTX displayed a high cytotoxicity, similar to free PTX with a high concentration. For example, A549 cell viability was 38.6% for 80 nM of free PTX while it was 38.4% GO-PEG/PTX with just 40 nM of PTX; MCF-7 cell viability was 16.4% for 80 nM of free PTX while it was 12.9% GO-PEG/PTX with only 20 nM of PTX. These results indicated that we could use GO-PEG nanocarrier to load low concentration of PTX for achieving the same treatment using higher concentration of free PTX. That is to say, GO-PEG nanocarrier could improve drug efficacy without increasing the chemotherapeutic drug dose.

Furthermore, we also investigated the cytotoxicity of GO-PEG/PTX and free PTX with same PTX concentration (40 nM) at different times from 12 to 72 h, as shown in Figure 9C,D. Both free PTX and GO-PEG/PTX inhibited A549 and MCF-7 cells in a time-dependent mode. For each time point, GO-PEG/PTX distinctly showed a higher cytotoxicity effect on tumor cell compared to free PTX. The increased cytotoxicity can be attributed to enhanced PTX cellular uptake when loaded on GO-PEG. It was also found that GO-PEG/PTX exhibited similar cytotoxicity in comparison with that of free PTX at shorter incubation time. For instance, A549 cell viability after incubating with free PTX for 72 h was 66.9%, while GO-PEG/PTX only spent 24 h to reach this value (68.0%) and the cell viability was as low as 31.6% after 72 h, which was much lower than that of free PTX; MCF-7 cell viability after incubating with free PTX for 72 h was 20.3%, while GO-PEG/PTX only spent 48 h to reach this value (22.0%) and the cell viability was as low as 10.2% after 72 h, which was much lower than that of free PTX. The result meant that GO-PEG could load PTX to achieve a faster treatment compared to that of free PTX so as for improving drug efficiency.

CONCLUSIONS

In the current work, GO-PEG was prepared by covalently grafting well-defined 6-armed PEG-NH_2 onto the surface of GO sheets via facile amidation and it was used as a nanocarrier to deliver a water-insoluble anticancer drug of PTX. The grafted PEG polymeric chains increased the physiological stability and biocompatibility of GO sheets and the nanocarrier was not cytotoxic by itself. The fluorescence cellular imaging of GO-PEG mixing with FITC confirmed that the nanocarrier could readily enter A549 and MCF-7 cells. GO-PEG could efficiently bind 11.2 wt % of PTX via $\pi-\pi$ stacking and hydrophobic interactions. WST-8 based colorimetric assay demonstrated that GO-PEG/PTX inhibited A549 and MCF-7 cells in a concentration- and time-dependent manner, and it exhibited a higher cytotoxicity effect compared to free PTX, especially at low concentration and short time, for improving the bioavailability of PTX. On the basis of aforementioned results, PEG-functionalized GO, GO-PEG, could be a promising nanomaterial in biological and medical areas.

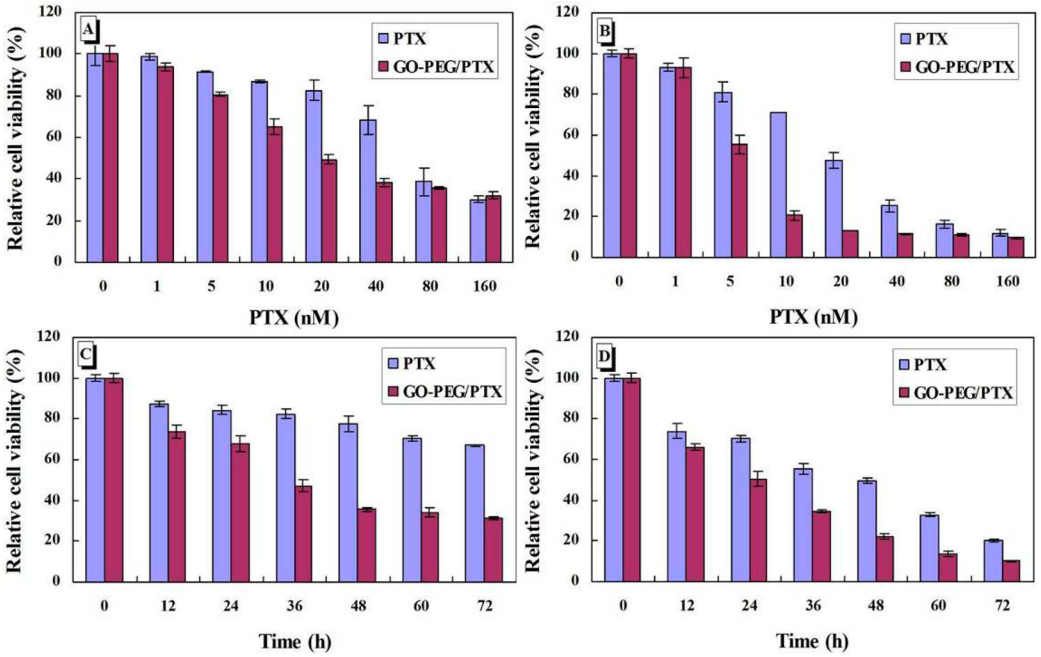

Figure 9. Relative cell viability of cells after treatment with different concentrations of PTX and GO-PEG/PTX for 72 h, (A) A-549 and (B) MCF-7; with different time at a constant PTX concentration of 40 nM, (C) A-549 and (D) MCF-7. The experiments were repeated three times, all with similar results. The data are presented as the mean ± SD (for each group, n = 3).

AUTHOR INFORMATION

Corresponding Authors

*Tel: +86-21-54925310; fax: +86-21-64166128; e-mail: xyhuang@mail.sioc.ac.cn.

*Tel: +86-21-64251655; fax: +86-21-64252920; e-mail: ship@ecust.edu.cn .

*Tel: +86-21-54925309; fax: +86-21-64166128; e-mail: liyongjun78@sioc.ac.cn.

Notes

The authors declare no competing financial interest.

ACKNOWLEDGMENTS

The authors are thankful for the financial support of the National Natural Science Foundation of China (21204098, 31100549, and 11275050), Shanghai Scientific and Technological Innovation Project (11nm0501100, 11ZR1445900, 14520720100, and 14520720700), State Key Laboratory of Bioreactor Engineering (2060204), and Fundamental Research Funds for the Central Universities (222201313010). We thank Prof. Guowei Wang (Fudan Univeristy) for assistance in synthesizing 6-armed PEG.

REFERENCES

(1) Novoselov, K. S.; Geim, A. K.; Morozov, S. V.; Jiang, D.; Zhang, Y.; Dubonos, S. V.; Grigorieva, I. V.; Firsov, A. A. Electric Field Effect in Atomically Thin Carbon Films. *Science* **2004**, *306*, 666−669.

(2) Geim, A. K. Graphene: Status and Prospects. *Science* **2009**, *324*, 1530−1534.

(3) Rao, C. N. R.; Sood, A. K.; Subrahmanyam, K. S.; Govindaraj, A. Graphene: The New Two-Dimensional Nanomaterial. *Angew. Chem., Int. Ed.* **2009**, *48*, 7752−7777.

(4) Fang, M.; Wang, K. G.; Lu, H. B.; Yang, Y. L.; Nutt, S. Covalent Polymer Functionalization of Graphene Nanosheets and Mechanical Properties of Composites. *J. Mater. Chem.* **2009**, *19*, 7098−7105.

(5) Zhang, Y. B.; Tan, Y. W.; Stormer, H. L.; Kim, P. Experimental Observation of the Quantum Hall Effect and Berry's Phase in Graphene. *Nature* **2005**, *438*, 201−204.

(6) Balandin, A. A.; Ghosh, S.; Bao, W.; Calizo, I.; Teweldebrhan, D.; Miao, F.; Lau, C. N. Superior Thermal Conductivity of Single-Layer Graphene. *Nano Lett.* **2008**, *8*, 902−907.

(7) Huang, X.; Qi, X.; Boey, F.; Zhang, H. Graphene-Based Composites. *Chem. Soc. Rev.* **2012**, *41*, 666−686.

(8) Li, X.; Wang, X.; Zhang, L.; Lee, S.; Dai, H. J. Chemically Derived, Ultrasmooth Graphene Nanoribbon Semiconductors. *Science* **2008**, *319*, 1229−1232.

(9) Sun, X. M.; Liu, Z.; Welsher, K.; Robinson, J. T.; Goodwin, A.; Zaric, S.; Dai, H. J. Nano-Graphene Oxide for Cellular Imaging and Drug Delivery. *Nano Res.* **2008**, *1*, 203−212.

(10) He, Q. Y.; Sudibya, H. G.; Yin, Z. Y.; Wu, S. X.; Li, H.; Boey, F.; Huang, W.; Chen, P.; Zhang, H. Centimeter-Long and Large-Scale Micropatterns of Reduced Graphene Oxide Films: Fabrication and Sensing Applications. *ACS Nano* **2010**, *4*, 3201−3208.

(11) Tang, L. A. L.; Wang, J.; Loh, K. P. Graphene-Based SELDI Probe with Ultrahigh Extraction and Sensitivity for DNA Oligomer. *J. Am. Chem. Soc.* **2010**, *132*, 10976−10977.

(12) Wang, Z.; Zhang, J.; Chen, P.; Zhou, X.; Yang, Y.; Wu, S.; Niu, L.; Han, Y.; Wang, L.; Chen, P.; Boey, F.; Zhang, Q.; Liedberg, B.; Zhang, H. Label-free, Electrochemical Detection of Methicillin-Resistant *Staphylococcus aureus* DNA with Reduced Graphene Oxide-Modified Electrodes. *Biosens. Bioelectron.* **2011**, *26*, 3881−3886.

(13) He, S.; Song, B.; Li, D.; Zhu, C.; Qi, W.; Wen, Y.; Wang, L.; Song, S.; Fang, H.; Fan, C. A Graphene Nanoprobe for Rapid, Sensitive, and Multicolor Fluorescent DNA Analysis. *Adv. Funct. Mater.* **2010**, *20*, 453−459.

(14) Liu, Z.; Robinson, J. T.; Sun, X. M.; Dai, H. J. PEGylated Nanographene Oxide for Delivery of Water-Insoluble Cancer Drugs. *J. Am. Chem. Soc.* **2008**, *130*, 10876−10877.

(15) Zhang, L. M.; Xia, J. G.; Zhao, Q. H.; Liu, L. W.; Zhang, Z. J. Functional Graphene Oxide as a Nanocarrier for Controlled Loading and Targeted Delivery of Mixed Anticancer Drugs. *Small* **2010**, *6*, 537−544.

(16) He, H. Y.; Klinowski, J.; Forster, M.; Lerf, A. A New Structural Model for Graphite Oxide. *Chem. Phys. Lett.* **1998**, *287*, 53−56.

(17) Yang, H. F.; Shan, C. S.; Li, F. H.; Han, D. X.; Zhang, Q. X.; Niu, L. Covalent Functionalization of Polydisperse Chemically-Converted Graphene Sheets with Amine-terminated Ionic Liquid. *Chem. Commun.* **2009**, 3880−3882.
(18) Yang, K.; Wan, J. M.; Zhang, S. A.; Zhang, Y. J.; Lee, S. T.; Liu, Z. In Vivo Pharmacokinetics, Long-Term Biodistribution, and Toxicology of PEGylated Graphene in Mice. *ACS Nano* **2011**, *5*, 516−522.
(19) Wang, K.; Ruan, J.; Song, H.; Zhang, J.; Wo, Y.; Guo, S.; Cui, D. X. Biocompatibility of Graphene Oxide. *Nanoscale Res. Lett.* **2011**, *6*, 8.
(20) Zhang, Y. B.; Ali, S. F.; Dervishi, E.; Xu, Y.; Li, Z. R.; Casciano, D.; Biris, A. S. Cytotoxicity Effects of Graphene and Single-Wall Carbon Nanotubes in Neural Phaeochromocytoma-Derived PC12 Cells. *ACS Nano* **2010**, *4*, 3181−3186.
(21) Deng, Y.; Li, Y. J.; Dai, J.; Lang, M. D.; Huang, X. Y. Functionalization of Graphene Oxide towards Thermo-Sensitive Nanocomposites via Moderate in Situ SET-LRP. *J. Polym. Sci., Part A: Polym. Chem.* **2011**, *49*, 4747−4755.
(22) Deng, Y.; Li, Y. J.; Dai, J.; Lang, M. D.; Huang, X. Y. An Efficient Way to Functionalize Graphene Sheets with Presynthesized Polymer via ATNRC Chemistry. *J. Polym. Sci., Part A: Polym. Chem.* **2011**, *49*, 1582−1590.
(23) Ma, X. X.; Tao, H. Q.; Yang, K.; Feng, L. Z.; Cheng, L.; Shi, X. Z.; Li, Y. G.; Guo, L.; Liu, Z. A Functionalized Graphene Oxide-Iron Oxide Nanocomposite for Magnetically Targeted Drug Delivery, Photothermal Therapy, and Magnetic Resonance Imaging. *Nano Res.* **2012**, *5*, 199−212.
(24) Zhang, B. W.; Zhang, Y. J.; Peng, C.; Yu, M.; Li, L. F.; Deng, B.; Hu, P. F.; Fan, C. H.; Li, J. Y.; Huang, Q. Preparation of polymer decorated graphene oxide by γ-ray induced graft polymerization. *Nanoscale* **2012**, *4*, 1742−1748.
(25) Prentice, D. E.; Majeed, S. K. Oral Toxicity of Polyethylene Glycol (PEG 200) in Monkeys and Rats. *Toxicol. Lett.* **1978**, *2*, 119−122.
(26) Leung, H. W.; Ballantyne, B.; Hermansky, S. J.; Franta, S. W. Peroral Subchronic, Chronic Toxicity, and Pharmacokinetic Studies of a 100-KiloDalton Polymer of Ethylene Oxide (Polyox N-10) in the Fischer 344 Rat. *Int. J. Toxicol.* **2000**, *19*, 305−312.
(27) Torchilin, V. P.; Omelyanenko, V. G.; Parisov, M. I.; Bogdanov, A. A.; Trubetskoy, V. S.; Herron, J. N.; Gentry, C. A. Poly(ethylene glycol) on the Liposome Surface: on the Mechanism of Polymer-Coated Liposome Longevity. *Biochim. Biophys. Acta* **1994**, *1195*, 11−20.
(28) Zalipsky, S. Chemistry of Polyethylene Glycol Conjugates with Biologically Active Molecules. *Adv. Drug Delivery Rev.* **1995**, *16*, 157−182.
(29) Yamaoka, T.; Tabata, Y.; Ikada, Y. Distribution and Tissue Uptake of Poly(ethylene glycol) with Different Molecular Weights after Intravenous Administration to Mice. *J. Pharm. Sci.* **1994**, *83*, 601−606.
(30) Zhang, M.; Li, X. H.; Gong, Y. D.; Zhao, N. M.; Zhang, X. F. Properties and Biocompatibility of Chitosan Films Modified by Blending with PEG. *Biomaterials* **2002**, *23*, 2641−2648.
(31) Wu, H. X.; Liu, G.; Zhang, S. J.; Shi, J. L.; Zhang, L. X.; Chen, Y.; Chen, F.; Chen, H. R. Biocompatibility, MR Imaging and Targeted Drug Delivery of a Rattle-type Magnetic Mesoporous Silica Nanosphere System Conjugated with PEG and Cancer-Cell-Specific Ligands. *J. Mater. Chem.* **2011**, *21*, 3037−3045.
(32) Yang, X. Y.; Zhang, X. Y.; Liu, Z. F.; Ma, Y. F.; Huang, Y.; Chen, Y. S. High-Efficiency Loading and Controlled Release of Doxorubicin Hydrochloride on Graphene Oxide. *J. Phys. Chem. C* **2008**, *112*, 17554−17558.
(33) Huizing, M. T.; Misser, V. H.; Pieters, R. C.; ten Bokkel Huinink, W. W.; Veenhof, C. H.; Vermorken, J. B.; Pinedo, H. N.; Beijnen, J. H. Taxanes: A New Class of Antitumor Agents. *Cancer Invest.* **1995**, *13*, 381−404.
(34) Smith, D. C.; Chay, C. H.; Dunn, R. L.; Fardig, J.; Esper, P.; Olson, K. Phase II Trial of Paclitaxel, Estramustine, Etoposide, and Carboplatin in the Treatment of Patients with Hormone-Refractory Prostate Carcinoma. *Cancer* **2003**, *98*, 269−276.
(35) Singla, A. K.; Garg, A.; Aggarwal, D. Paclitaxel and Its Formulations. *Int. J. Pharm.* **2002**, *235*, 179−192.
(36) Jin, J. Y.; Lee, W. S.; Joo, K. M.; Maiti, K. K.; Biswas, G.; Kim, W.; Kim, K. T.; Lee, S. J.; Kim, K. H.; Nam, D. H.; Chung, S. K. Preparation of Blood-brain Barrier-permeable Paclitaxel-carrier Conjugate and Its Chemotherapeutic Activity in the Mouse Glioblastoma Model. *Med. Chem. Commum.* **2011**, *2*, 270−273.
(37) Rele, S. M.; Cui, W. X.; Wang, L. C.; Hou, S. J.; Barr-Zarse, G.; Tatton, D.; Gnanou, Y.; Esko, J. D.; Chaikof, E. L. Dendrimer-like PEO Glycopolymers Exhibit Anti-Inflammatory Properties. *J. Am. Chem. Soc.* **2005**, *127*, 10132−10133.
(38) Mei, B. C.; Susumu, K.; Medintz, I. L.; Delehanty, J. B.; Mountziaris, T. J.; Mattoussi, H. Modular Poly(ethylene glycol) Ligands for Biocompatible Semiconductor and Gold Nanocrystals with Extended pH and Ionic Stability. *J. Mater. Chem.* **2008**, *18*, 4949−4958.
(39) Liu, J. H.; Chen, G. S.; Jiang, M. Supramolecular Hybrid Hydrogels from Noncovalently Functionalized Graphene with Block Copolymers. *Macromolecules* **2011**, *44*, 7682−7691.
(40) Li, L. L.; Tang, F. Q.; Liu, H. Y.; Hao, N. J.; Chen, D.; Teng, X.; He, J. Q. In Vivo Delivery of Silica Nanorattle Encapsulated Docetaxel for Liver Cancer Therapy with Low Toxicity and High Efficacy. *ACS Nano* **2010**, *4*, 6874−6882.
(41) Peng, C.; Hu, W.; Zhou, Y.; Fan, C. H.; Huang, Q. Intracellular Imaging with a Graphene-Based Fluorescent Probe. *Small* **2010**, *6*, 1686−1692.
(42) Cauda, V.; Schlossbauer, A.; Kecht, J.; Zurner, A.; Bein, T. Multiple Core-Shell Functionalized Colloidal Mesoporous Silica Nanoparticles. *J. Am. Chem. Soc.* **2009**, *131*, 11361−11370.
(43) Yang, K.; Zhang, S.; Zhang, G. X.; Sun, X. M.; Lee, S. T.; Liu, Z. Graphene in Mice: Ultrahigh In Vivo Tumor Uptake and Efficient Photothermal Therapy. *Nano Lett.* **2010**, *10*, 3318−3323.